Journal of Applied Polymer Science

Preparation and properties of polyurethane-modified epoxy cured in different simulated gravity environments

Defeng Li,[1] Youshan Wang,[2] Yuyan Liu,[1] Zhimin Xie,[2] Lei Wang,[1] Huifeng Tan[2]

[1]School of Chemical Engineering and Technology, Harbin Institute of Technology, Harbin 150001, China

[2]National Key Laboratory of Science and Technology on Advanced Composites in Special Environments, Harbin Institute of Technology, Harbin 150001, China

Correspondence to: Y. Wang (E-mail: wangys@hit.edu.cn) and Y. Liu (E-mail: liuyy@hit.edu.cn)

ABSTRACT: Great attention has been paid to the composites with interpenetrating polymer networks (IPNs) because of their special performance. However, the influence of sedimentation and convection from different gravity environments on the formation of IPNs and the properties of IPNs blends has received little attention. To understand their influence, environments with different gravity accelerations of 0*g*, 1*g*, and 2*g* were simulated with a superconducting magnet, and tests, including differential scanning calorimetry (DSC), dynamic mechanical analysis (DMA), coefficient of thermal expansion (CTE), scanning electron microscopy, and three-point bending, of the IPNs blends cured in different gravity environments were conducted and analyzed. Fourier transform infrared spectroscopy, DSC, and DMA proved the formation of IPNs during the reaction between the polyurethane prepolymer (PUP) and epoxy resin (E51). The curves of DSC also certified the differences in the curing degree between the different parts along the direction of gravity of a sample. With the increase of mass fraction of PUP, the change trends of the storage modulus presented a linear decrease when samples cured in microgravity environment, but presented a parabolic trend when samples were cured in terrestrial environment. The damping properties of samples cured in simulated microgravity environments are better than those cured in terrestrial environment. With the increase in the simulated acceleration of gravity, the diameter of dispersed phase in a sea-island structure increased, but their number decreased and the bending stress and CTE of the IPN blends all decreased. These results show the formation of IPNs was affected by different gravity values, and the thermal and mechanical properties of the IPN composites were influenced by the changed IPN components. © 2015 Wiley Periodicals, Inc. J. Appl. Polym. Sci. **2015**, *132*, 42063.

KEYWORDS: blends; composites; copolymers; crosslinking; synthesis and processing

Received 21 September 2014; accepted 31 January 2015

DOI: 10.1002/app.42063

INTRODUCTION

Epoxy resins (EP) are considered one of the most important thermosetting polymers; they are widely used as adhesives, sealants, surface coatings, printed circuit boards, electric encapsulating materials, damping materials, manufacture of microdevices, and matrices for high-performance composites because of their excellent properties of adhesion, thermostability, creep resistance, high strength and stiffness, chemical corrosion resistance, electrically insulating properties, dimensional stability, and simplicity in processing.[1–11] Unfortunately, because of their high crosslinking density, the cured EPs exhibit low impact strength, poor crack resistance, and small elongation at break; that is, these defects make them brittle and limit their applications as engineering materials.[1,3–5,12–14]

In the past few decades, a considerable amount of work has been devoted to improving the fracture toughness and mechanical properties of EP; these include the incorporation of particulate fillers, reactive liquid rubbers, and thermoplastic polymers into the epoxy matrix.[15–19] Some of the toughening approaches, such as the addition of rubber, have led to the deterioration of the mechanical and thermal properties of EP. To overcome the drawbacks, ductile thermoplastics, such as polyurethane prepolymer (PUP), have been used to toughen EPs.[3,20–23] PUP is one of the most commonly used additions to improve the elasticity and toughness of epoxy resin because of its flexible chains and excellent elasticity. EP/PUP systems have been reported many times because of their excellent performance generated by the interpenetrating polymer networks (IPNs) in the systems.[24]

The system with IPNs is a special polymer blend consisting of at least two polymers in a molecular network, which is kept together by permanent entanglement, with excellent thermal stability and mechanical properties caused by synergistic effects of each component.[25,26] The EP/PUP IPNs blends and their

modifications have been paid much attention, especially their mechanical and thermal conductivity properties.[27–31] The properties of blends with IPNs are significantly determined by the grafted structure of IPNs, and they are influenced when the grafted structure of IPNs is changed. Microgravity is one of the factors affecting the structure of IPNs.

A microgravity environment is one special environment with an acceleration of gravity less than $10^{-4}g$,[32] which can be obtained by freefall, drop shaft, parabolic flight, and space station experiments,[33–35] or simulated by rotary cell culture systems and a random positioning machine.[36–38] In a terrestrial gravity environment, the gravity obviously influences the sedimentation of polymeric microgels, the convection of heat and concentration, and the temperature gradient,[39–42] whereas in the microgravity environment, these phenomena will disappear.[43] The space environment is a typical microgravity environment, and polymer polymerization has been confirmed that it is the best way to fabricate the hard structure in a space environment because this method can break up the limits of structure and size of the space environment laboratory and the space station by the advantages of its lightweight and portability.[44,45] However, the properties of IPNs cured in space environment will be different from those cured in an terrestrial environment because the formation and development of IPNs are all related to the phenomena of sedimentation and concentration. Researchers[46,47] have reported that the properties of the curing product, especially big-scale resin materials, are influenced by the curing environment, such as the heat concentration generated by the sedimentation and concentration from the environment.

In this study, a superconducting magnet (JASTEC-16T) was used to simulate the different gravity environments (0*g*, 1*g*, and 2*g*), with the superiorities of cost-effectiveness, long lifetime, and independence from liquid conditions. The feasibility of this equipment has already been verified, on the basis of which some research on life science and material science have been conducted.[48–50]

Herein, environments with gravity accelerations of 0*g*, 1*g*, and 2*g* were simulated by a superconducting magnet. The tests, including differential scanning calorimetry (DSC), dynamic mechanical analysis (DMA), coefficient of thermal expansion (CTE), scanning electron microscopy (SEM), and three-point bending, of the EP/PUP blends cured in different gravity environments were conducted. The molecular chain networks and microgel generated during the formation of IPNs were all sensitive to gravity; if the movement of molecular chain networks and microgel changed with the gravity, how did the IPNs and properties of materials with IPNs change? We discuss that in this work, and the research conclusions can be good guidance for the manufacturing of excellent blends with IPNs in terrestrial environment and the application of blend with IPNs used in different gravity environments in the future.

EXPERIMENTAL

Raw Materials

Bisphenol A glycidyl ether epoxy resin E51, with an epoxy value of 0.5 ± 0.01 and a type of WSR618, was purchased from Wuxi Resin Factory of Bluestar New Chemical Materials Co., Ltd. (Jiangsu, China).

The curing agent was a modified amine (named 593, Shanghai Resin Factory Co., Ltd., Shanghai, China). It was a transparent liquid and had long chain structures; the viscosity of it was 80–100 mPa s (298.15 K).

PUP was purchased from Jiangyan Hengchuang Insulation Materials Co., Ltd. (Hubei, China). The average molecular weight was 2600–2700, and the content of the active group (NCO) was 0.07 mol/100 g.

Simulation Equipment

The superconducting magnet used in our experiments and associated information are shown in Figure 1. The magnet could simulate three different gravity environments with gravitational accelerations of 0*g*, 1*g*, and 2*g*; the corresponded to the magnetic field strength of 9, 16, and 12 T, respectively. The magnetic strength of superconducting magnet was about five orders of magnitude higher than that of the ground (0.5×10^{-4} T). The four gravity environments, including terrestrial 1*g* and simulated 0*g*, 1*g*, and 2*g* are abbreviated to G, G0, G1, and G2, respectively, for simplicity.

Sample Preparation

The calculated amount of PUP was added to the heated resin at about 70°C, and then, the mixtures were stirred vigorously with mechanical stirring for 30 min at 70°C to ensure the uniformity. The homogeneous mixtures were cooled to room temperature, and certain proportion of curing agent was added to the mixtures. This was followed by the blending of the EP/PUP/593 mixture according to the same steps as the preparation of the EP/PUP system. The mixture was degassed *in vacuo* and poured into the four gravity environments, G, G0, G1, and G2, with an environmental temperature of 40°C. The ratios of PUP to EP were 10/100 (denoted as 10 wt % for facility), 15/100 (15 wt %), 20/100 (20 wt %), and 25/100 (25 wt %), respectively. To explore the influences of different gravities on the properties of different parts of one sample, each sample was cut into upper and lower parts to compare their properties. The cutting method was the same as our previous report.[51] Briefly, the height of the sample was 8 mm, and the location of 4 mm was selected as the cutting position. Then, the upper and lower parts were obtained.

Characterization

The IR spectra of the samples were recorded with an Equinox 55 Fourier transform infrared (FTIR) spectrophotometer (Bruker, Germany) over the range of 4000–400 cm^{-1} at a resolution of 4 cm^{-1}.

DSC was done by a STARe system analyzer (Mettler Toledo, Switzerland) at a 10°C/min heating rate under the nitrogen flow rate of 30 mL/min from 0 to 200°C.

The thermomechanical properties, including the modulus and glass-transition temperatures (T_g's), were tested with DMA (SDTA861e, Mettler Toledo) under a shear mode over a temperature range from 25 to 130°C at a heating rate of 5°C/min with

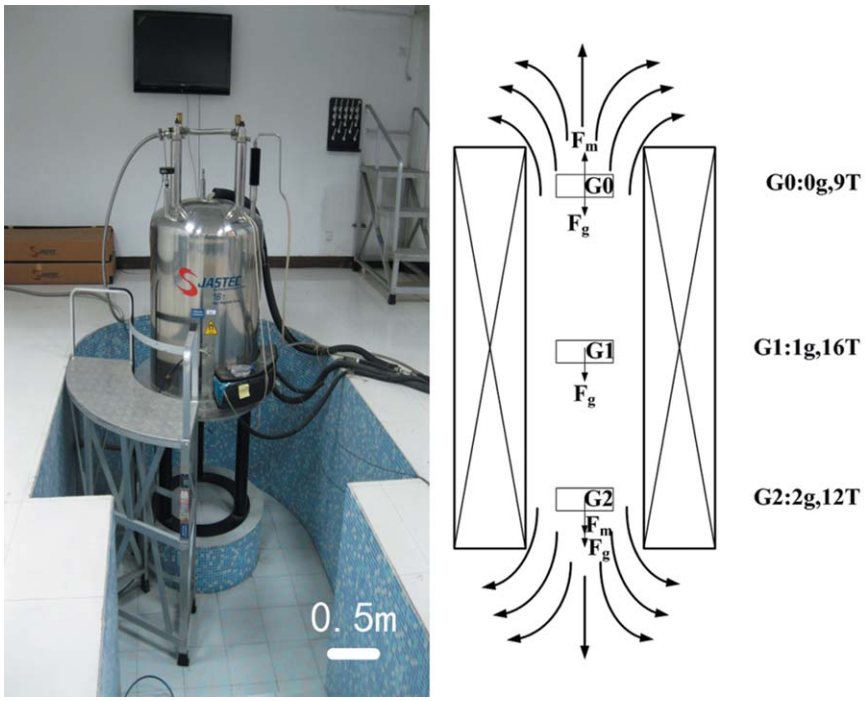

Figure 1. Photograph of the superconducting magnet and its associated information. F_m, magnetic field force; F_g, gravitational force. [Color figure can be viewed in the online issue, which is available at wileyonlinelibrary.com.]

a frequency of 1 Hz, an amplitude of 3 μm, a force of 5 N, and a sample size of diameter, $\Phi = 10 \times 3.4$ mm^2.

Thermogravimetric analysis (TGA) was determined by a TGA/DSC STARe system (Mettler Toledo) with a heating rate 10°C/min from 30 to 700°C under a nitrogen atmosphere.

CTE was measured by a TMA/SDTA840 instrument (Mettler Toledo) at a heating rate of 5°C/min from room temperature to 200°C with a sample size of $\Phi = 10 \times 3.4$ mm^2.

The flexural properties were measured on an Instron 5965 universal material tester (Instron) at room temperature with a crosshead speed of 2 mm/min. We obtained all of the data by testing samples (35 mm×7 mm×3.4 mm) for three times.

The morphology of the fracture surfaces was observed by a Helios Nanolab600i electronic microscope (FEI). The specimen surfaces were coated with a thin gold film to increase their conductance for SEM observation.

RESULTS AND DISCUSSION

FTIR Spectroscopy

FTIR spectrum analysis is a major method for investigating the curing mechanism and structural changes of the EP/PU mixture. The FTIR spectra of E51, PUP, PUP + E51, and PUP + E51 + 593 (cured in G) are shown in Figure 2. It is clear that there were characteristic peaks of —NCO (2270 cm^{-1}) and C═O (1727 cm^{-1}) in curve a, and the —OH (3500 cm^{-1}) and epoxy groups (916 cm^{-1}) in curve b. PUP and E51 reacted under stirring for 30 min at 70°C to form the product of PUP + E51. The characteristic peak of —OH (3500 cm^{-1}) disappeared in curve c; this indicated the reaction between the isocyanate group in the PUP and hydroxyl groups in E51, where the latter was consumed completely in this reaction. At the same time, the isocyanate group in PUP also reacted with the epoxy group in E51; this could be certified by the weakened characteristic peaks of the epoxy group (916 cm^{-1}) and ether linkage (1038 and 1183 cm^{-1}).[3,52–54] In the two previous reactions, the mixing molecule networks were formed between PUP and E51; this resulted from the intertwinement with each other and the chemical reaction. This played an important role in the formation of IPNs between the EP/PU mixture and 593. The epoxy group (916 cm^{-1}) almost disappeared in curve d; this means that the epoxy group from the EP/PU mixture reacted

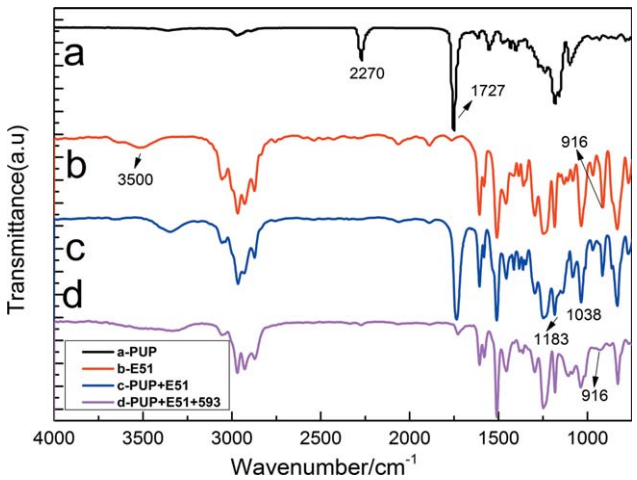

Figure 2. FTIR spectra of (a) PUP, (b) E51, (c) PUP + E51, and (d) PUP + E51 + 593. [Color figure can be viewed in the online issue, which is available at wileyonlinelibrary.com.]

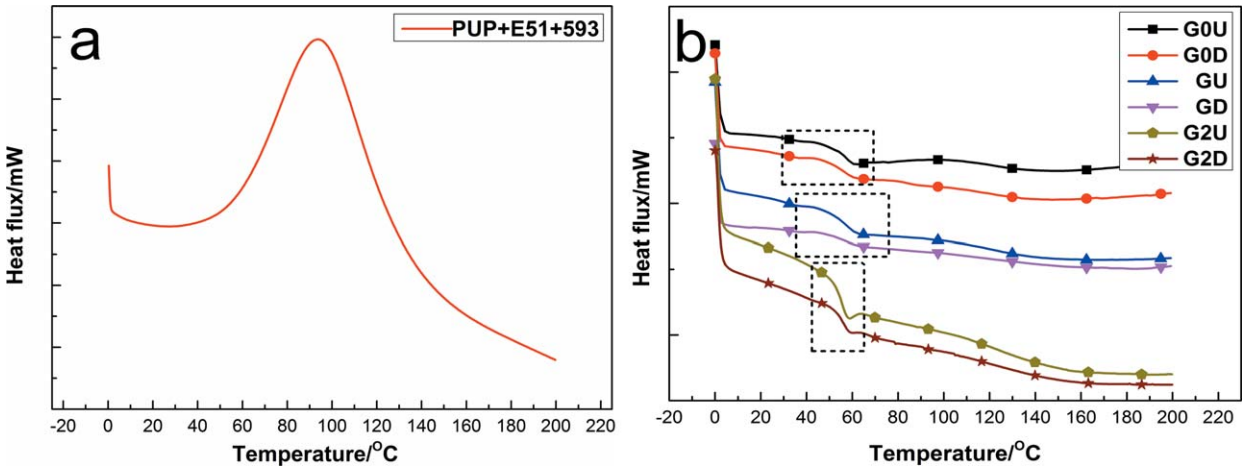

Figure 3. Exothermic curves of (a) a PUP + E51 + 593 blend with 20 wt % PUP cured in G and (b) upper (U) and lower (D) parts of the blend cured in G0, G, and G2. G0U, the tested specimen is the upper part of the sample cured in the G0 environment; G1U, the tested specimen is the upper part of the sample cured in the G1 environment; G2U, the tested specimen is the upper part of the sample cured in the G2 environment. [Color figure can be viewed in the online issue, which is available at wileyonlinelibrary.com.]

with the amino group of 593. Along with the reaction between the epoxy and amino groups, the IPNs formed gradually.

DSC

Information about the tested systems, such as the heat release, T_g, and phase structure of the multiphase system, could be obtained by the monitoring of the exothermic curve of DSC. Figure 3(a) shows the exothermic curve of the PUP + E51 + 593 blend with 20 wt % PUP. There is only one peak in this curve, and it exhibits considerable compatibility between PUP and EP in the IPNs.[55,56]

Figure 3(b) shows the exothermic curves of the PUP + E51 + 593 blend cured in G0, G, and G2. The curves of the upper and lower part of one sample are abbreviated as U and D in the figure. As is shown in Figure 3(b), when the sample was cured in the same environment, T_g of the lower part was slightly higher than that of upper part. The difference was the smallest when the samples were cured in G0 and largest when the samples were cured in G2. When the samples were cured in G or G2, the sedimentation effect made the intertwined segments and microgels sink down to the bottom of the sample and triggered the heat concentration,[57] which promoted the reactions in the lower part of the sample and made the curing degree in the lower part higher than that in the upper part.[51,58] However, when the samples were cured in G0, the whole sample cured at uniform curing rate and had the same curing degree because of the disappearance of the sedimentation effect.[51,59] There were small exothermic peaks in the curves of the upper part after T_g because of the lack of postcuring. The exothermic peak area decreased with the growth of gravity; this indicated that different gravity values had effects on the curing degree.

DMA

The dynamic storage modulus (E') reflects the load-bearing capacity of the materials. Figure 4 shows the curves of E' of the blends with different PUP mass fractions cured in G and G0.

When the samples were cured in G and G0, respectively, the E' values of the blends were lower than those of the pure epoxy.

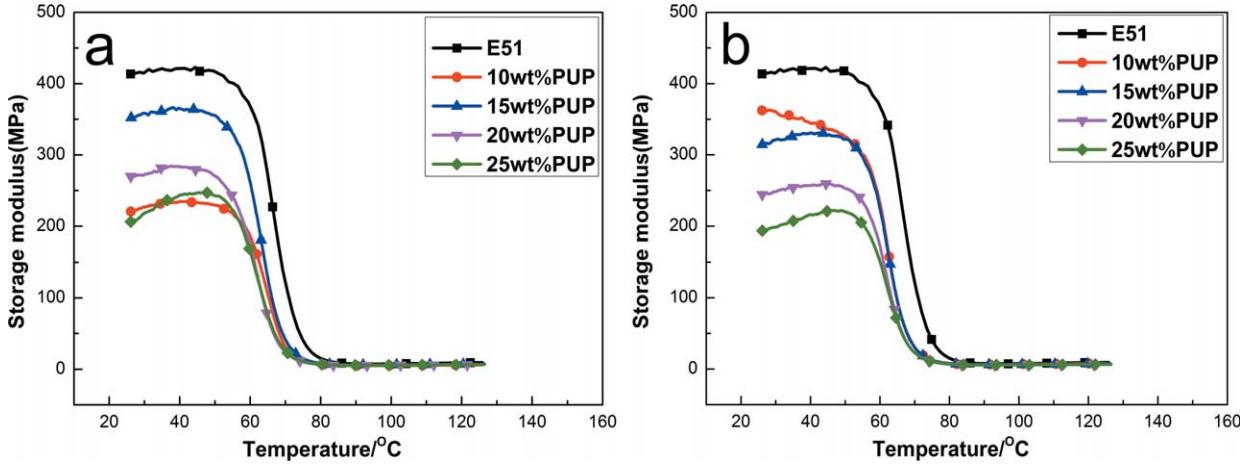

Figure 4. E' curves of blends with different PUP mass fractions cured in (a) G and (b) G0. [Color figure can be viewed in the online issue, which is available at wileyonlinelibrary.com.]

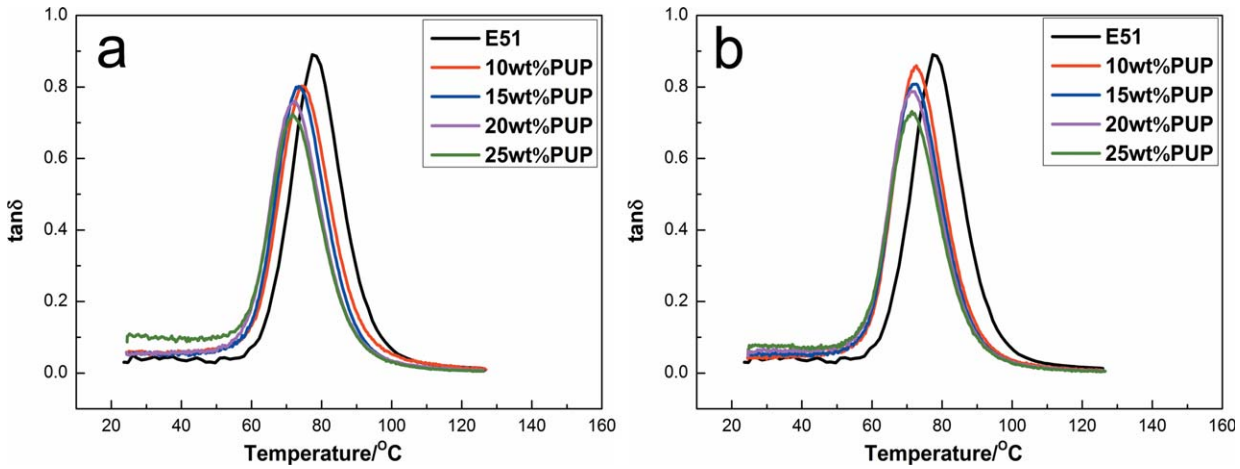

Figure 5. Tan δ curves of the blends with different PUP mass fractions cured in (a) G and (b) G0. [Color figure can be viewed in the online issue, which is available at wileyonlinelibrary.com.]

The PUP contained flexible segments and active carboxyls, but because the activity of the carboxyls was weaker than that of the hydroxyls in the epoxy, the reaction between the carboxyls and curing agent 593 became difficult. The combined effect of both the flexible segments and unreacted carboxyls in the blend made the segment move more freely and made the crosslinking density decrease. This caused E' of the blend to decline. The decreasing trends of E' were different in G and G0. In G [Figure 4(a)], there was an increasing trend first and a decline in the following part during the addition of PUP. E' was the highest when the addition amount of PUP was 15 wt %. The changing tendency of E' was the same as in the bending stress test in the previous part of this study. In G0 [Figure 4(b)], E' decreased linearly with the addition of PUP. The nonlinear decline of E' in G resulted from effects of the sedimentation and convection generated by gravity, which made the IPNs distribute chaotically in the blend. Meanwhile, when cured in G0, the curing behavior of the blend was closer to the theoretical value, and E' of the blend showed a linear decline because of the disappearance of sedimentation and convection. The difference in E' of the samples with the same addition amount of PUP was not large; this was mainly because the sample size was small, and the influences of sedimentation and convection were not obvious.

The analysis of the curve of the loss tangent (tan δ; defined by the ratio of loss modulus (E'') to storage modulus (E') is an important method of DMA because it shows information such as the damping capability (dissipation of the vibration energy) and T_g, wherein the temperature range of tan $\delta > 0.3$ has been always used to analyze the damping capability of materials. The curves and characteristic data of the PUP-modified epoxy are shown in Figure 5 and Table I, respectively.

When the blends were incorporated with different mass fractions of PUP cured in G and G0, their T_g values both decreased a little with increasing PUP content from 10 to 25 wt %; this was in agreement with other studies.[60] The incorporation of flexible segments decreased the volume fraction of rigid segments in both environments. Cured in the same environment, the blends with PUP contents of 10 and 15 wt % all had good damping properties, but the damping properties of the samples cured in G0 were better than the properties of those cured in G. The friction among the segments of the IPNs influenced the damping properties of the materials.[61] As mentioned previously, when cured in a gravity environment, the EP/PUP networks could not be uniformly distributed in the uncured blend because of the sedimentation and convection from gravity, whereas they were uniformly distributed when cured in a microgravity environment because of the disappearance of sedimentation and convection. The homogeneous EP/PUP networks generated homogeneous IPNs, which promoted the friction and winding among the segments[62] and also improved the damping properties by increasing the energy dissipation of the blend.

TGA

Figure 6(a) shows the thermal stability of E51 blends with 10 and 25 wt % PUP. In the blend, there were two kinds of segmental networks. One was generated by the reaction between 593 and epoxy, and the other was generated by the reaction between 593 and flexible segments of PUP. The IPNs were generated by the two kinds of networks through chemical reactions and intertwined in the blends. Because of the existence of the

Table I. Characteristic DMA Data for Modified Epoxy Cured in G and G0 with Different Mass Fractions of PUP

	PUP/blend (%)	Tan $\delta > 0.3$ (°C)	Tan δ (maximum)	T_g (°C)
G	0 (pure E51)	68–90	0.89	77
	10	65–86	0.80	74
	15	64–84	0.80	74
	20	63–83	0.76	72
	25	63–83	0.72	72
G0	10	63–84	0.86	73
	15	63–83	0.81	73
	20	62–83	0.79	72
	25	62–82	0.73	71

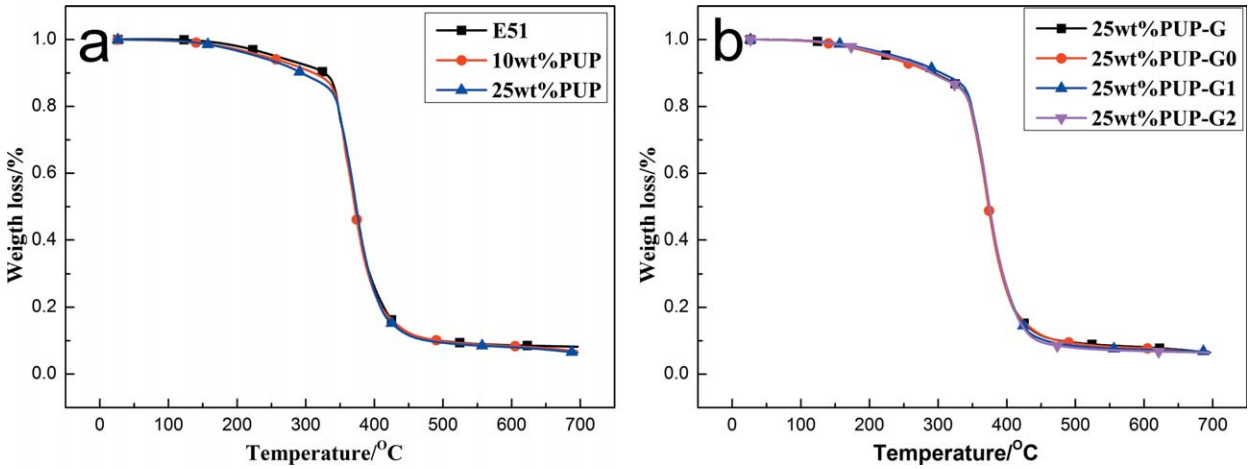

Figure 6. Thermal stability of the (a) E51 and mixtures with different mass fractions of PUP cured in G and (b) mixtures with 25 wt % PUP cured in different environments. [Color figure can be viewed in the online issue, which is available at wileyonlinelibrary.com.]

aromatic ring in the epoxy, the cured epoxy had a high crosslinking density, and the motion of the segments was difficult. This made the epoxy possess a good thermal stability. Compared to the epoxy, PUP had more flexible segments, which endowed them with poor thermal stability. So, the thermal stability of the mixture with epoxy and PUP decreased with increasing mass fraction of PUP. As the mechanism of thermal decomposition of the EP/PU system,[63] before 350°C, the thermal decomposition was mainly that of urethane and aromatic linkage from PUP, and after 350°C, the remaining ingredients of the system were essentially the same as that of the pure epoxy. Hence, the thermal decomposition rate of the EP/PU system increased with increasing mass fraction of PUP before 350°C and almost did not change after 350°C. The change trend of the thermal decomposition rate shown in Figure 6(a) was accordance with the decomposition mechanism.

Figure 6(b) shows the thermal degradation properties of blends with 25 wt % PUP cured in four different gravity environments. The curves indicate that the thermal stability of the blends with IPNs was almost not affected by the different gravity values; this might have been because the different gravity values only changed the uniformity rather than the molecular structure of the IPNs blends.

CTE

The influences of different environments and the mass fraction of PUP on the thermal expansion of the modified epoxy could be analyzed through a comparison of the CTE values of different specimens. The CTE value is directly related to the crosslink density and free volume properties of epoxy systems;[64] when the crosslink is bigger, the free volume is smaller. With eq. (1) for the CTE value,[65] we calculated the values of the samples cured in different environments and obtained Figure 7:

$$\alpha = (1/L_0)(\Delta L/\Delta T) \quad (1)$$

where α is the CTE value, L_0 is the initial dimension, ΔL is the change in length, and ΔT is the change in temperature.

The CTE value after T_g was higher than that before T_g for the same sample, just as is shown in Figure 7; this was caused by different intermolecular forces under different temperatures. In

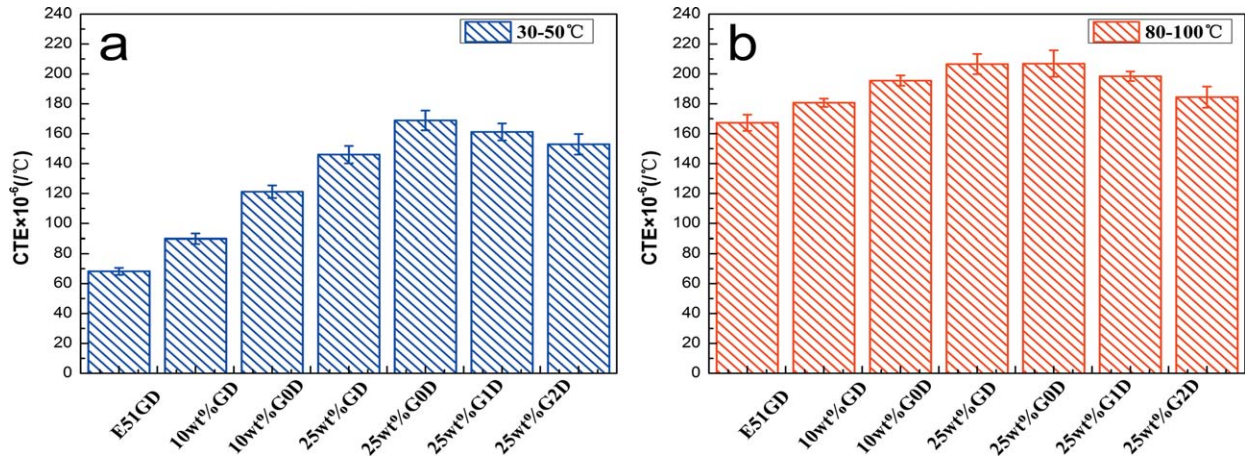

Figure 7. CTE values of different systems cured in different gravity environments: (a) before T_g and (b) after T_g. [Color figure can be viewed in the online issue, which is available at wileyonlinelibrary.com.]

Table II. Bending Stress of Epoxy Modified with Different Mass Fractions of PUP Cured in Different Environments

	G (MPa)	G0 (MPa)	G1 (MPa)	G2 (MPa)	(G – G2)/G (%)
E51	143	142	139	135	5.6
10% PUP	92	92	90	87	5.4
15% PUP	102	97	93	90	11.8
20% PUP	94	89	87	83	11.7
25% PUP	86	81	78	74	14.0

the temperature range higher than T_g, the intermolecular distance increased because the molecular vibrations became stronger. When the blends had different mass fractions of PUP (E51 GD, 10 wt % GD, and 25 wt % GD), their CTE values increased with increasing added amount of PUP. When we added more PUP into the mixture, there were more flexible segments and a corresponding reduction in the volume fraction of the rigid aromatic rings in the mixture; this reduced the resistance of expansion when the segments were heated and made the expansion behavior more likely to occur.

The CTE value decreased with increasing gravity value (25 wt % PUP cured in GD, G0D, G1D, and G2D). The CTE values before and after T_g in G2 were reduced by 9.5 and 10.8%, respectively, compared to those of the samples cured in G0. This could be explained as follows. When the uncured EP + PUP + 593 blend into was placed into the different curing environments, when there was a sinking force generated by gravity, just like in G and G2, the EP/PUP networks sank down and reacted with 593 to form the IPNs in the bottom of the sample. This made the crosslinking density in the lower part of the sample higher than the average value of the whole sample. If there was no sinking force, just like in G0, the reaction proceeded uniformly and the crosslinking density of the lower part of the sample was just the average value. The crosslinking density in the lower part of the sample increased with the augment of sinking force. Because the sinking force increased with the gravity value, the crosslinking density in the lower part of the sample rose with increasing gravity value. The CTE value decreased with increasing crosslinking density, so the CTE values decreased with the rise of gravity values.

Three-Point Bending Testing

As shown in Table II, in each one of the four environments, the bending stress of the PUP-modified epoxy was the smallest compared to all of those of the other pure epoxy. The addition of flexible segments of PUP reduced the volume fraction of the rigid aromatic rings in the blend, and this led to a reduction in the bending stress. The reduction first increased and then decreased; this was because when the PUP was blended into the mixture, the IPNs became compact by chemical reaction and intertwined with the chains of PUP. If the mass fraction of PUP went over 15 wt %, the volume friction of flexible segments in

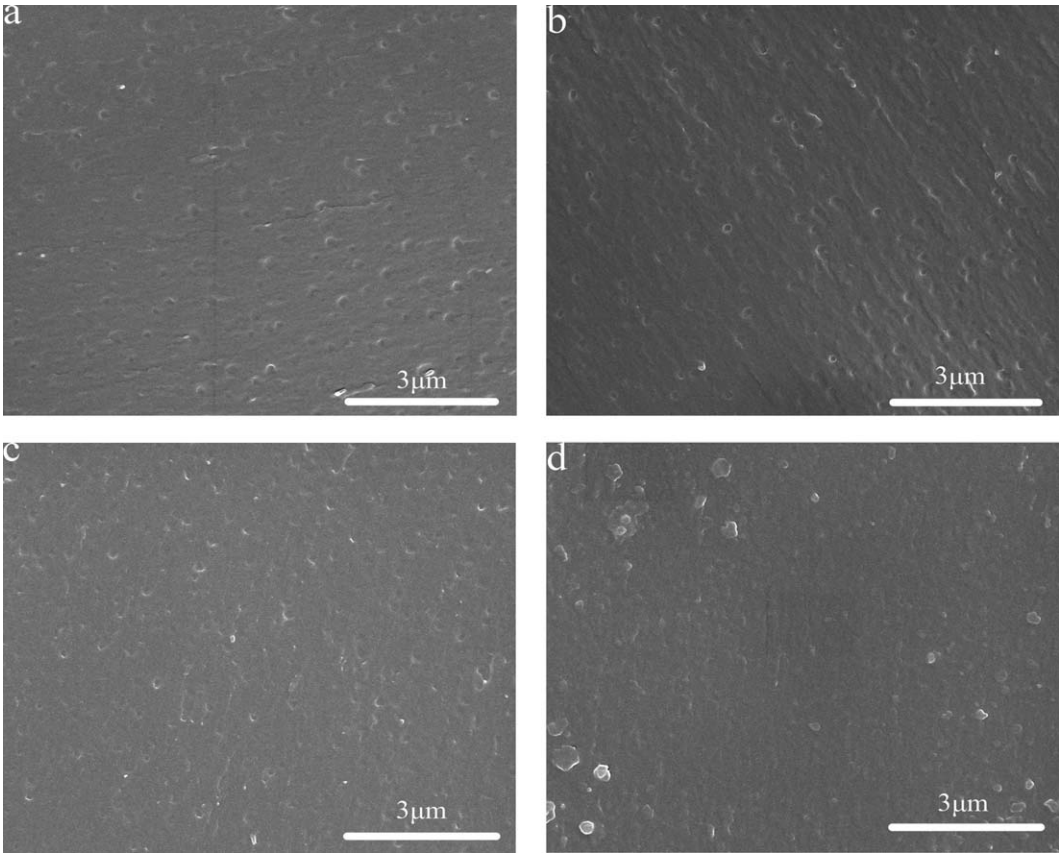

Figure 8. SEM images of 15 wt % PUP-modified epoxy cured in (a) G, (b) G0, (c) G1, and (d) G2.

the mixture were so high that it made the crosslinking density decrease and caused a decline in the bending stress.

The average bending stress of the samples cured in G was the biggest compared to those of samples cured in the other three simulated environments. Compared with the three simulated environments, the bending stress decreased with increasing simulated gravity value and mass fraction of PUP. When the mass fraction of PUP was 25 wt %, the bending stress of the samples cured in G2 decreased by 14% compared to that of the samples cured in G. As stated previously, the magnetic strength of a superconducting magnet is about five orders of magnitude higher than that in the ground, and this might have changed the uniformity of the IPNs and made the IPN blends cured in it have a reduced bonding stress.

SEM

Because of the excellent bending stress of the blend with 15 wt % PUP, the microstructures of the 15 wt % PUP-modified epoxy cured in different gravity environments were tested. The sea-island structure (SIS) could clearly observed, as shown in Figure 8(a) (G). The dispersed phase was uniformly distributed in the continuous phase of the matrix. These flexible dispersed phase increased the fracture toughness of the blend not only by changing the direction of crack propagation but also by absorbing the energy of crack propagation.[7] In the SIS system, the properties of the dispersed phase, such as the volume, density, and uniformity of dispersion, directly affected the toughening effects. There were a large number of islands, shown in Figure 8(b) (G0), and they were all uniformly dispersed in the resin matrix. With increasing gravity value, the number of islands decreased slightly, as shown in Figure 8(c) (G1). The dispersed phase with a smaller diameter aggregated and combined into a dispersed phase with larger diameter in the bottom of the sample, as shown in Figure 8(d) (G2); this reduced the interaction between the dispersed phase and the continuous phase by decreasing the contact area between the two phases. At the same time, the dispersed phase with a large diameter easily created phase separation with the continuous phase, and this significantly reduced the mechanical properties of the material.

CONCLUSIONS

In this article, the PUP-modified epoxy was prepared in different gravity environments, and the properties of the modified epoxy were investigated, and we drew the following conclusions:

1. The formation of IPNs in the reaction between PUP and E51 was proven by the analysis of FTIR spectroscopy, DSC, and DMA. Different parts along the direction of gravity of one sample had different curing degrees; this was certified by the DSC analysis.
2. With increasing mass fraction of polyurethane, the E' values of the samples cured in a microgravity environment presented a linear decrease, but when the samples were cured in a terrestrial environment, their decrease in E' showed a parabolic trend. The damping properties of the samples cured in simulated microgravity environments were better than those of the samples cured in a terrestrial environment.
3. With increasing simulated acceleration of gravity, the diameter of the dispersed phase in SIS increased, but the number of them decreased, and the bending stress and CTE values of the IPN blends all decreased. When the mass friction of PUP was 25 wt %, the average values of the bending stress and CTE of the samples cured in simulated supergravity environments decreased by 8.6 and 10.8%, respectively, compared to those of the samples cured in simulated microgravity environments.

ACKNOWLEDGMENTS

This work was financially supported by the Fundamental Research Funds for the Central Universities (contract grant number HIT.-KISTP.201408), the Program for Harbin City Science and Technology Innovation Talents of the Special Fund Project (contract grant number 2012RFXXG091), and the Preresearch Fund Project of National Defense.

REFERENCES

1. Ban, J. F.; Lu, S. R.; Guo, D.; Liu, K.; Luo, C. X. *Adv. Mater. Res.* **2011**, *194*, 1421.
2. Kostrzewa, M.; Hausnerova, B.; Bakar, M.; Siwek, E. *J. Appl. Polym. Sci.* **2011**, *119*, 2925.
3. Bakar, M.; Duk, R.; Przybylek, M.; Kostrzewa, M. *J. Reinforced Plast. Compos.* **2008**, *28*, 2107.
4. Song, J.; Chen, G.; Ding, Y.; Shi, J.; Liu, Y.; Li, Q. *Polym. Int.* **2011**, *60*, 1594.
5. Bakar, M.; Kostrzewa, M.; Hausnerova, B.; Sar, K. *Adv. Polym. Technol.* **2010**, *29*, 237.
6. Fu, H.; Huang, H.; Wang, Q.; Zhang, H.; Chen, H. *J. Dispersion Sci. Technol.* **2009**, *30*, 634.
7. Lu, S.; Ban, J.; Yu, C.; Deng, W. *Iranian Polym. J.* **2010**, *19*, 669.
8. Wang, L.; Ma, S.; Wang, X. J.; Bi, H.; Han, X. *J. Asia-Pacific J. Chem. Eng.* **2014**, *9*, 877.
9. Saadati, P.; Baharvand, H.; Rahimi, A.; Morshedian, J. *Iranian Polym. J.* **2005**, *14*, 637.
10. Wei, C.; Tan, S. T.; Wang, X. Y.; Zhang, M. Q.; Zeng, H. M. *J. Mater. Sci. Lett.* **2002**, *21*, 719.
11. Khurana, P.; Aggarwal, S.; Narula, A. K.; Choudhary, V. *Polym. Int.* **2003**, *52*, 908.
12. Siddhamalli, S. K. *Polym. Compos.* **2000**, *21*, 846.
13. Yee, A. F.; Pearson, R. A. *J. Mater. Sci.* **1986**, *21*, 2462.
14. Naffakh, M.; Dumon, M.; Gerard, J. *Compos. Sci. Technol.* **2006**, *66*, 1376.
15. Bakar, M.; Wojtania, I.; Legocka, I.; Gospodarczyk, J. *Adv. Polym. Technol.* **2007**, *26*, 223.
16. Chikhi, N.; Fellahi, S.; Bakar, M. *Eur. Polym. J.* **2002**, *38*, 251.
17. Frigione, M.; Acierno, D.; Mascia, L. *Adv. Polym. Technol.* **1999**, *18*, 237.
18. Pearson, R. A.; Yee, A. F. *J. Mater. Sci.* **1991**, *26*, 3828.
19. Spanoudakis, J.; Young, R. J. *J. Mater. Sci.* **1984**, *19*, 473.

20. Hedrick, J. L.; Yilgor, I.; Jurek, M.; Hedrick, J. C.; Wilkes, G. L.; McGrath, J. E. *Polymer* **1991**, *32*, 2020.
21. Rong, M. Z.; Zeng, H. M. *Polymer* **1997**, *38*, 269.
22. Bucknall, C. B.; Partridge, I. K. *Polymer* **1983**, *24*, 639.
23. Hourston, D. J.; Lane, J. M.; MacBeath, N. A. *Polym. Int.* **1991**, *26*, 17.
24. Frisch, H. L.; Frisch, K. C.; Klempner, D. *Polym. Eng. Sci.* **1974**, *14*, 646.
25. Sanchez, M. S.; Ferrer, G. G.; Cabanilles, C. T.; Duenas, J. M. M.; Pradas, M. M.; Ribelles, J. L. G. *Polymer* **2001**, *42*, 10071.
26. Frounchi, M.; Burford, R. P.; Chaplin, R. P. *Polymer* **1994**, *35*, 5073.
27. Romanes, M. C.; D'Souza, N. A.; Coutinho, D.; Balkus, K. J.; Scharf, T. W. *Wear* **2008**, *265*, 88.
28. Cristea, M.; Ibanescu, S.; Cascaval, C. N.; Rosu, D. *High Perform. Polym.* **2009**, *21*, 608.
29. Chen, S.; Wang, Q.; Pei, X.; Wang, T. *J. Appl. Polym. Sci.* **2010**, *118*, 1144.
30. Merlin, D. L.; Sivasankar, B. *Eur. Polym. J.* **2009**, *45*, 165.
31. Ye, Y.; Chen, H.; Wu, J.; Ye, L. *Polymer* **2007**, *48*, 6426.
32. Tsuchida, A.; Taguchi, K.; Takyo, E.; Yoshimi, H.; Kiriyama, S.; Okubo, T.; Ishikawa, M. *Colloid Polym. Sci.* **2000**, *278*, 872.
33. Langevin, D.; Vignes-Adler, M. *Eur. Phys. J. E* **2014**, *37*, 16.
34. Sakuma, G.; Fukunaka, Y.; Matsushima, H. *Int. J. Hydrogen Energy* **2014**, *39*, 7638.
35. Tsuchida, A.; Yoshimi, H.; Kiriyama, S.; Ohiwa, K.; Okubo, T. *Colloid Polym. Sci.* **2003**, *281*, 760.
36. Sokolovskaya, A. A.; Ignashkova, T. I.; Bochenkova, A. V.; Moskovtsev, A. A.; Baranov, V. M.; Kubatiev, A. A. *Acta Astronautica* **2014**, *99*, 16.
37. Freed, L. E.; Hollander, A. P.; Martin, I.; Barry, J. R.; Langer, R.; Vunjak-Novakovic, G. *Exp. Cell Res.* **1998**, *240*, 58.
38. Infanger, M.; Kossmehl, P.; Shakibaei, M.; Baatout, S.; Witzing, A.; Grosse, J.; Bauer, J.; Cogoli, A.; Faramarzi, S.; Derradji, H.; Neefs, M.; Paul, M.; Grimm, D. *Apoptosis* **2006**, *11*, 749.
39. Briskman, V.; Kostarev, K.; Yudina, T.; Levtov, V.; Romanov, V. *AIAA* **1995**, *0263*, 1.
40. Briskman, V.; Kostarev, K.; Levtov, V.; Lyubimova, T.; Mshinsky, A.; Nechitailo, G.; Romanov, V. *Acta Astronautica* **1996**, *39*, 395.
41. Briskman, V. A. *Adv. Space Res.* **1999**, *24*, 1199.
42. Sorrentino, L.; Tersigni, L. *Appl. Compos. Mater.* **2012**, *19*, 31.
43. Briskman, V. A.; Yudina, T. M.; Kostarev, K. G.; Kondyurin, A. V.; Leontyev, V. B.; Levkovich, M. G.; Mashinsky, A. L.; Nechitailo, G. S. *Acta Astronautica* **2001**, *48*, 169.
44. Kondyurin, A. *Adv. Space Res.* **2001**, *28*, 665.
45. Kondyurin, A.; Lauke, B.; Kondyurina, I.; Orba, E. *Adv. Space Res.* **2004**, *34*, 1585.
46. Briskman, V. A. *Adv. Space Res.* **1999**, *24*, 1199.
47. Sorrentino, L.; Tersigni, L. *Appl. Compos. Mater.* **2012**, *19*, 31.
48. Fujiwara, Y.; Katsumoto, Y.; Ohishi, Y.; Koyama, M.; Ohno, K.; Akita, M.; Inoue, K.; Tanimoto, Y. *J. Phys. Conf. Ser.* **2006**, *51*, 458.
49. Beaugnon, E.; Tournier, R. *Nature* **1991**, *349*, 6309.
50. Yin, D. C.; Lu, H. M.; Geng, L. Q.; Shi, Z. H.; Luo, H. M.; Li, H. S.; Ye, Y. J.; Guo, W. H.; Shang, P.; Wakayama, N. I. *J. Crystal Growth* **2008**, *310*, 1206.
51. Li, D. F.; Liu, Y. Y.; Wang, Y. S.; Kang, H. J.; Wang, L.; Tan, H. F. *J. Appl. Polym. Sci.* **2015**, *132*, 41413.
52. Deka, H.; Karak, N. *Polym. Adv. Technol.* **2011**, *22*, 973.
53. Li, Z. H.; Huang, Y. P.; Ren, D. Y.; Zheng, Z. Q. *J. Central South Univ. Technol.* **2008**, *15*, 305.
54. Bakar, M.; Kostrzewa, M. *J. Thermoplast. Compos. Mater.* **2009**, *23*, 749.
55. Kalita, H.; Karak, N. *Des. Monomers Polym.* **2013**, *16*, 447.
56. Lu, S. R.; Ban, J. F.; Yu, C. H.; Deng, W. X. *Iranian Polym. J.* **2010**, *19*, 669.
57. Briskman, V.; Kostarev, K.; Levtov, V.; Lyubimova, T.; Mashinsky, A.; Nechitailo, G.; Romanov, V. *Acta Astronautica* **1996**, *39*, 395.
58. Briskman, V. A.; Yudina, T. M.; Kostarev, K. G.; Kondyurin, A. V.; Leontyev, V. B.; Levkovich, M. G.; Mashinsky, A. L.; Nechitailo, G. S. *Acta Astronautica* **2001**, *48*, 169.
59. Fujiwara, Y.; Katsumoto, Y.; Ohishi, Y.; Koyama, M.; Ohno, K.; Akita, M.; Inoue, K.; Tanimoto, Y. *J. Phys. Conf. Ser.* **2006**, *51*, 458.
60. Chen, S.; Wang, Q.; Wang, T. *High Perform. Polym.* **2011**, *23*, 345.
61. Chen, S.; Wang, Q.; Wang, T. *Polym. Test.* **2011**, *30*, 726.
62. Wang, Q.; Chen, S.; Wang, T.; Zhang, X. *Appl. Phys. A* **2010**, *104*, 375.
63. Semsarzadeh, M. A.; Navarchian, A. H. *J. Appl. Polym. Sci.* **2003**, *90*, 963.
64. Wang, B.; Gong, W.; Liu, W. H.; Wang, Z. F.; Qi, N.; Li, X. W.; Liu, M. J.; Li, S. *J. Polymer* **2003**, *44*, 4047.
65. Rahman, M. M.; Hosur, M.; Ludwick, A. G.; Zainuddin, S.; Kumar, A.; Trovillion, J.; Jeelani, S. *Polym. Test.* **2012**, *31*, 777.